ULTRA WIDEBAND WIRELESS COMUNICATIONS IN THE 60 GHz BAND

Y. PINHASI [1•], A. YAHALOM[1], G.A. PINHASI[2], M. LUTVAK[1]
[1] Department of Electrical and Electronic Engineering
[2]Department of Chemical Engineering and Biotechnology
Ariel University Center of Samaria
P.O. Box 3, Ariel 40700,
ISRAEL
yosip@ariel.ac.il www.ariel.ac.il/sites/yosip/

Abstract: - The growing demand for broadband wireless communication links and the lack of wide frequency bands within the conventional spectrum causes us to seek bandwidth in the higher microwave and millimeter-wave spectrum at Extremely High Frequencies (EHF) above 30GHz. One of the principal challenges in realizing modern wireless communication links in the EHF band is phenomenon occurring during electromagnetic wave propagation through the atmosphere. Space-frequency theory of the propagation of an ultra-wide band radiation in dielectric media is presented. Characterization of the atmospheric medium is via its refractivity leading to a transfer function, which describes the response of the medium in the frequency domain. This description enables the consideration of broadband signals taking into account inhomogeneous absorptive and dispersive effects of the medium. Analytical expressions are derived when a pulse-modulated signal is propagating in a general dielectric material. We demonstrate the approach by studying propagation of ultra-wide band signals, while transmitted in the vicinity of the 60GHz absorption peak of the atmospheric medium at millimeter wavelengths.

Key-Words: - Ultra-wide Band, Extremely high frequencies, Broadband wireless communications, Atmosphere

1 Introduction

The growing demand for broadband wireless communication links and the deficiency of wide frequency bands within the conventional spectrum, require utilization of higher microwave and millimeter-wave spectrum at the Extremely High Frequencies (EHF) above 30GHz. In addition to the fact that the EHF band (30-300GHz) covers a wide range, which is relatively free of spectrum users, it offers many advantages for wireless communication and RADAR systems. Among the practical advantages of using the EHF region for satellite communications systems is the ability to employ smaller transmitting and receiving antennas. This allows the use of a smaller satellite and a lighter launch vehicle

Some of the principal challenges in realizing modern wireless communication links at the EHF band are the effects emerging when the electromagnetic radiation propagates through the atmosphere. Figure 1 is a schematic illustration of a wireless communication line-of-sight (LOS) link, where the atmospheric medium is described by the transfer function $H(jf)$.

When millimeter-wave radiation passes through the atmosphere, it suffers from selective molecular absorption [1-6]. Several empirical and analytical models were suggested for estimating the millimeter and infrared wave transmission of the atmospheric medium.

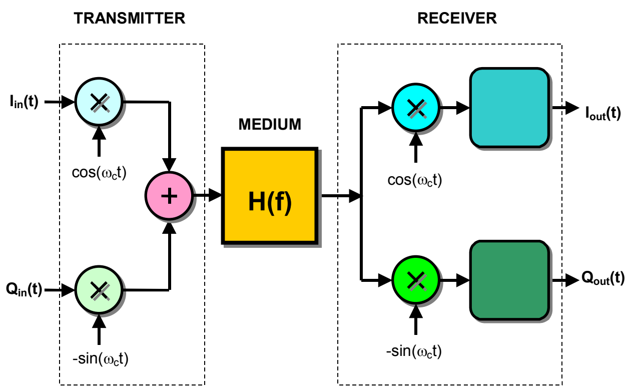

Figure 1: Wireless communication link.

• Corresponding author: E – mail: yosip@ariel.ac.il

The transmission characteristics of the atmosphere at the EHF band, as shown in Figure 2 was calculated with the millimeter propagation model (MPM), developed by Liebe [7-10]. Curves are drawn for several values of relative-humidity (RH), assuming clear sky and no rain. Inspection of Figure 2 reveals absorption peaks at 22GHz and 183GHz, where resonance absorption of water (H_2O) occurs, as well as absorption peaks at 60GHz and 119GHz, due to absorption resonances of oxygen (O_2). Between these frequencies, minimum attenuation is obtained at 35GHz (Ka-band), 94GHz (W-band), 130GHz and 220GHz, which are known as atmospheric transmission 'windows' [4].

The inhomogeneous transmission in a band of frequencies causes absorptive and dispersive effects in the amplitude and in phase of wide-band signals transmitted in the EHF band. The frequency response of the atmosphere plays a significant role as the data rate of a wireless digital radio channel is increased. The resulting amplitude and phase distortion leads to inter-symbol interference, and thus to an increase in the bit error rate (BER). These effects should be taken into account in the design of broadband communication systems, including careful consideration of appropriate modulation, equalization and multiplexing techniques.

In this paper, we develop a general space-frequency approach for studying wireless communication channels operating in the EHF band. The theory is used to compare between analytical and numerical models. The constraints of the derived analytical expressions are discussed, pointing out conditions of validity. The MPM model [7-8] is used in the numerical model for calculation of atmospheric characteristics in the frequency domain. The resulting propagation factor is calculated numerically, enabling one to deal with ultra-wide band arbitrary signals.

The theory was used to study the effects of the atmospheric medium on a radio link, shown in Figure 1. The data signal, represented by a complex envelope $A_{in}(t)=I_{in}(t)-jQ_{in}(t)$, modulates a carrier wave at frequency f_c. The resultant signal is transmitted and propagates to the receiver site through the atmosphere along a line-of-sight path. The demodulated in-phase $I_{out}(t)$ and quadrature $Q_{out}(t)$ signals, retrieved at the receive outputs, are examined.

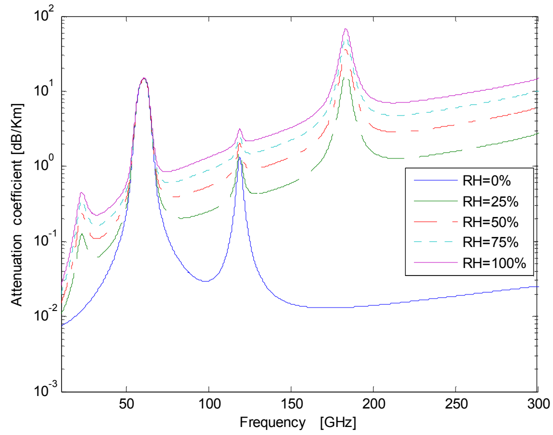

Figure 2: Millimeter wave attenuation coefficient $20\log(e)\alpha(f)$ in [dB/Km] for various values of relative humidity (RH).

The application of the model is demonstrated on a wireless data link operating in the 60GHz band. The unused frequency space and the high attenuation due to oxygen absorption (-15dB/Km) [11-14] make this frequency range naturally fitting for local broadband digital networks with small reuse distances [14]. The effects predicted by the analytical derivation are inspected in the numerical simulations, including the evolution of pulse distortion along the path of propagation in the atmospheric medium. The numerical model enables consideration of further ultra-short pulses, enduring very few carrier periods; such situations cannot be treated with the aid of analytical approximated derivations.

2 Millimeter Wave Propagation in the Atmosphere

The time dependent field $E(t)$ represents an electromagnetic wave propagating in a medium. The Fourier transform of the field is:

$$\mathbf{E}(f)=\int_{-\infty}^{+\infty} E(t)e^{-j2\pi ft}dt \tag{1}$$

In the far field, transmission of a wave, radiated from a localized (point) isotropic source and propagating in a (homogeneous) medium is characterized in the frequency domain by the transfer function:

$$H(jf)=\frac{\mathbf{E}_{out}(jf)}{\mathbf{E}_{in}(jf)} \propto e^{-jk(f)\cdot d} \tag{2}$$

here, $k(f)=2\pi f\sqrt{\mu\varepsilon}$ is a frequency dependent propagation factor, where ε and μ are the permittvity and the permeability of the medium, respectively. The transfer function $H(jf)$ describes the frequency response of the medium. In a dielectric medium the permeability is equal to that of the vacuum $\mu=\mu_0$ and the permittivity is given by $\varepsilon(f)=\varepsilon_r(f)\varepsilon_0$. If the medium introduces losses and dispersion, the relative dielectric constant $\varepsilon_r(f)$ is a complex, frequency dependent function. The resulting index of refraction can be presented by:

$$n(f)=\sqrt{\varepsilon_r(f)}=1+N(f)\times 10^{-6} \qquad (3)$$

where $N(f)=N_0+N'(f)-jN''(f)$ is the complex refractivity given in PPM [9]. The propagation factor can be written in terms of the index of refraction:

$$k(f)=\frac{2\pi f}{c}n(f)=\underbrace{-j\frac{2\pi f}{c}N''(f)\times 10^{-6}}_{\alpha(f)} \qquad (4)$$

$$\underbrace{+\frac{2\pi f}{c}\left(1+N_0\times 10^{-6}\right)+\overbrace{\frac{2\pi f}{c}N'(f)\times 10^{-6}}^{\Delta\beta(f)}}_{\beta(f)}$$

3 Transmission of Ultra-Wide Band Modulated Signal

Assume that a carrier wave at f_c is modulated by a wide-band signal $A_{in}(t)$:

$$E_{in}(t)=\mathrm{Re}\left\{A_{in}(t)e^{j2\pi f_c t}\right\} \qquad (5)$$

as shown in Figure 1. Here $A_{in}(t)=I_{in}(t)-jQ_{in}(t)$ is a complex envelope, representing the base-band signal, where $I_{in}(t)=\mathrm{Re}\{A_{in}(t)\}$ and $Q_{in}(t)=-\mathrm{Im}\{A_{in}(t)\}$ are the in-phase and the quadrature information waveforms respectively. The complex amplitude after propagation in the medium with the transfer function $H(jf)$ is calculated by [15]:

$$A_{out}(t)=\int_{-\infty}^{+\infty}\mathbf{A}_{in}(f)H(f+f_c)e^{+j2\pi ft}df \qquad (6)$$

where $\mathbf{A}_{in}(f)$ is the Fourier transform of $A_{in}(t)$. The above formalism, which is illustrated in a flowchart in Figure 3, is utilized in the followings for analytical derivation and numerical calculations of the demodulated signal at the receiver cite.

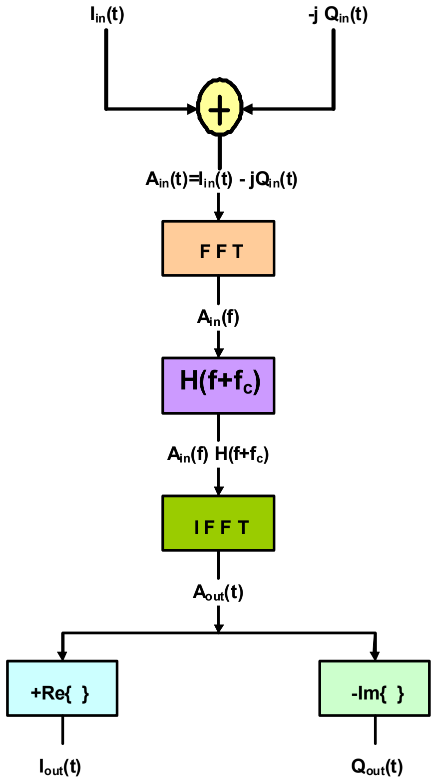

Figure 3: The procedure for calculation of de-modulated quadrature signals received in a wireless communication channel.

Now we assume that the transmitted waveform is a carrier modulated by a Gaussian envelope:

$$A_{in}(t)=e^{-\frac{t^2}{2\sigma_{in}^2}} \qquad (7)$$

characterized by a standard deviation σ_{in}. Fourier transformation of the pulse results in a Gaussian line-shape in the frequency domain:

$$\mathbf{A}_{in}(f)=\sqrt{2\pi}\sigma_{in}e^{-\frac{1}{2}(2\pi\sigma_{in}f)^2} \qquad (8)$$

shown in Figure 4. The corresponding standard deviation frequency bandwidth is $\sigma_f=1/(2\pi\sigma_{in})$. The full-width half-maximum (FWHM) is the –3dB bandwidth and is equal to $\mathrm{B}=2\sqrt{\ln(2)}\sigma_f\cong 0.265\sigma_{in}^{-1}$.

Analytical result of $A_{out}(t)$ after propagation along a horizontal path in the atmospheric medium can be found if the complex propagation factor $k(f)$ is approximated in the vicinity of the carrier frequency f_c, by a second order Taylor expansion:

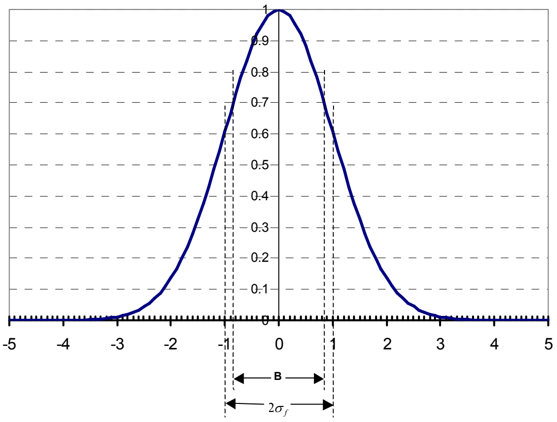

Figure 4: The normalized Gaussian lineshape.

$$k(f) \cong k_c + k'(f - f_c) + \frac{1}{2}k''(f - f_c)^2 \tag{9}$$

where

$$k_c \equiv k(f_c) \qquad k' \equiv \left.\frac{dk}{df}\right|_{f_c} \qquad k'' \equiv \left.\frac{d^2k}{df^2}\right|_{f_c}$$

resulting in a complex envelope:

$$A_{out}(t) = \frac{\sigma_{in}}{\sigma} e^{-\left(t - \frac{k'd}{2\pi}\right)^2 / 2\sigma^2} e^{-jk_c d} \tag{10}$$

where:

$$\sigma^2 = \sigma_{in}{}^2 + j\frac{k''}{(2\pi)^2} d \tag{11}$$

The expression (10) obtained for $A_{out}(t)$ is valid if:

$$\mathrm{Re}\{\sigma^2\} = \sigma_{in}{}^2 + \frac{\alpha'' d}{(2\pi)^2} > 0 \tag{12}$$

This condition is always satisfied if $\alpha'' > 0$. However, at frequencies for which the attenuation curve is convex $\alpha'' < 0$ (in the vicinity of the absorption lines) the analytical results are valid only for $\sigma_{in}{}^2 > -\alpha'' d/(2\pi)^2 > 0$. Another interpretation of this result is that for a given initial pulse width σ_{in}, the distance should not exceed $d < -(2\pi\sigma_{in})^2/\alpha''$. The magnitude (absolute value) of the complex envelope has a Gaussian shape:

$$|A_{out}(t)| = \frac{\sigma_{in}}{|\sigma|} e^{-\frac{(t-t_d)^2}{2\sigma_{out}{}^2}} \times \exp\left[-\alpha_0 d + \frac{1}{2}\frac{(\alpha' d)^2}{(2\pi\sigma_{in})^2 + \alpha'' d}\right] \tag{13}$$

with a temporal delay:

$$t_d = \frac{1}{2\pi}\left[\beta' - \frac{\alpha'\beta'' d}{(2\pi\sigma_{in})^2 + \alpha'' d}\right] d \tag{14}$$

and a standard deviation σ_{out} given by:

$$\sigma_{out}{}^2 = \sigma_{in}{}^2 + \frac{\alpha'' d}{(2\pi)^2} + \frac{\left[\beta'' d/(2\pi)^2\right]^2}{\sigma_{in}{}^2 + \alpha'' d/(2\pi)^2} \tag{15}$$

In the framework of the above approximation (9), a Gaussian magnitude $|A_{out}(t)| = \sqrt{I_{out}{}^2(t) + Q_{out}{}^2(t)}$ is preserved while propagating in the medium (although its width changes).

For a short distance (or a wide pulse), the time delay (14) can be approximated by $t_d \approx (\beta'/2\pi)d$. This becomes the exact solution at attenuation peaks, when $\alpha' = 0$.

Examination the expression (15) for σ_{out} reveals that when $\alpha'' \geq 0$ the pulse always widens along the path of propagation. However, for $\alpha'' < 0$ (e.g. in the vicinity of absorption frequencies), the pulse may become narrower while propagating in the atmospheric medium. Pulse compression occurs when $\sigma_{in}{}^2/d > -(\alpha''^2 + \beta''^2)/\left[(2\pi)^2\alpha''\right]$. For long propagation distances, the time delay approaches $t_d \to (\alpha''\beta' - \alpha'\beta'')d/(2\pi\alpha'')$ and the standard deviation $\sigma_{out}{}^2 \to (\alpha''^2 + \beta''^2)d/\left[(2\pi)^2\alpha''\right]$.

4 Pulse Propagation in a Resonant Medium

Some of dielectric media, such as gaseous ones, are characterized by resonant refractivity of the Lorentzian lineshape [16-17]:

$$N(f) = \frac{N_{DC}}{1 - (f/f_0)^2 + j(f_0/f)/Q} \tag{16}$$

where f_0 is the resonant frequency. The quality factor Q is a measure for how many periods the oscillations take the energy to dissipate. In that case one can write:

$$\alpha(f) = \frac{\alpha_0}{1 + Q^2(f/f_0 - f_0/f)^2} \tag{17}$$

$$\Delta\beta(f) = -Q\left(\frac{f}{f_0} - \frac{f_0}{f}\right)\alpha(f)$$

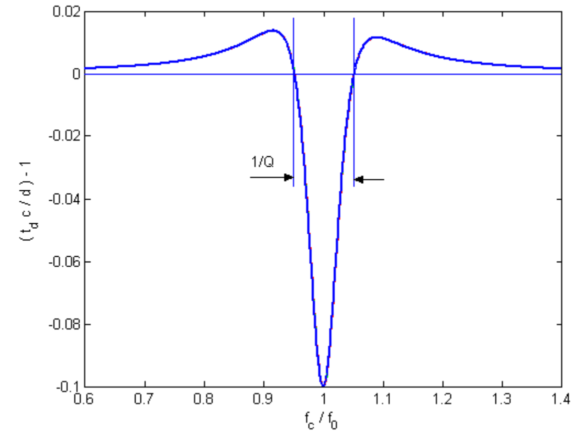

(*a*)

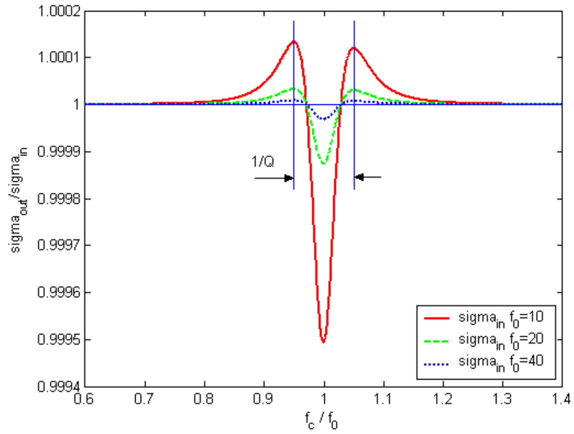

(*b*)

Figure 5: *a*) Delay time $\left[t_d-(d/c)\right]/(d/c)$, and *b*) pulse width σ_{out}/σ_{in} as a function of carrier frequency f_c for χ_{DC}=0.001 and Q=10 and several $\sigma_{in} f_0$.

Analytical derivations of the various pulse characteristics involve derivatives of up to the second order of the frequency dependent functions. The corresponding delay time t_d given and standard deviation σ_{out} of the pulse width are shown in Figure 5 for several initial pulse widths σ_{in}.

Examining Fig. 5.a for the time delay reveals that in the vicinity of resonant frequency f0, when the carrier frequency f_c is within the FWHM $\Delta f = f_0/Q$ of the resonance (i.e. $f_0-\Delta f/2 < f_c < f_0+\Delta f/2$), a signal Gaussian envelope arrives faster than should be expected by speed of light propagation; hence it appears super-luminal as previously expected. A minimum (super-luminal) delay is observed when the carrier frequency is equal to that of the resonance $f_c = f_0$, where the absorption peaks ($\alpha' = 0$). Maximum delays are found at $f_c \cong f_0\left[1\pm\sqrt{3}/(2Q)\right]$, where $\alpha'\beta''$ is most negative. Fig. 6.b shows that pulse compression is realized when $f_0\left[1-1/\left(2\sqrt{3}Q\right)\right] < f_c < f_0\left[1+1/\left(2\sqrt{3}Q\right)\right]$ where $\alpha'' < 0$ while maximum expansion occurs at $f_c \cong f_0\left[1\pm\sqrt{5}/2Q\right]$

Whe

If the carrier frequency is equal to that of the resonance, i.e. $f_c = f_0$, an expression for the the time delay is found to be:

$$t_d = \frac{1}{2\pi}\beta' \cdot d = \left(1-Q^2\cdot\chi_{DC}\right)\cdot\frac{d}{c} = \left(1-2Q\frac{\alpha_0}{\beta_0}\right)\cdot\frac{d}{c} \qquad (18)$$

The standard deviation of the pulse after propagation in the dielectric medium is:

$$\sigma_{out}^{\ 2} = \left[\sigma_{in}^{\ 2} - 2\left(\frac{Q}{\pi f_0}\right)^2 \alpha_0 d\right]\cdot\left\{1+\left[\frac{\frac{2\alpha_0 d}{Q}}{\left(2\pi\sigma_{in}\frac{f_0}{Q}\right)^2 - 8\alpha_0 d}\right]^2\right\} \qquad (19)$$

and the expected attenuation is:

$$Attenuation = \frac{\sigma_{in}^{\ 2}}{\left[\sigma_{in}^{\ 2} - 8\left(\frac{Q}{2\pi f_0}\right)^2 \alpha_0\cdot d\right]^2 + \left[\frac{2Q}{(2\pi f_0)^2}\alpha_0\cdot d\right]^2}\cdot e^{-2\alpha_0\cdot d} \qquad (20)$$

Graphs of calculation example of the group delay (18) and standard deviation (19) as a function of initial pulse duration σ_{in} are shown in Figure 6. A minimum delay is observed in Fig. 6.a when the carrier frequency is set to be $f_c = f_0$. A minimum pulse width is obtained in Fig. 6.b when $\sigma_{in}^{\ 2} = 2Q(4Q+1)\alpha_0 d/(2\pi f_0)^2$ resulting in $\sigma_{out_{\min}}^{\ 2} = Q\alpha_0 d/(\pi f_0)^2$.

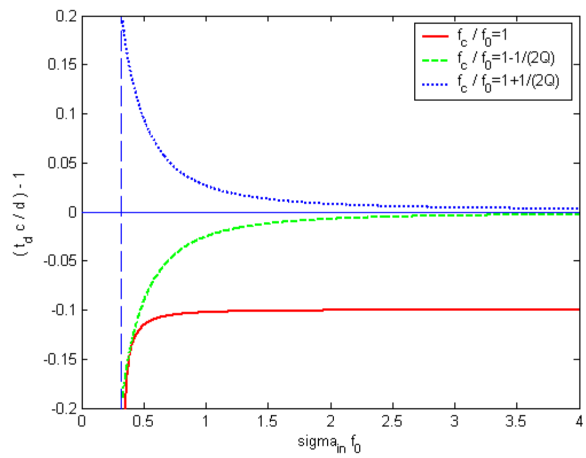

(*a*)

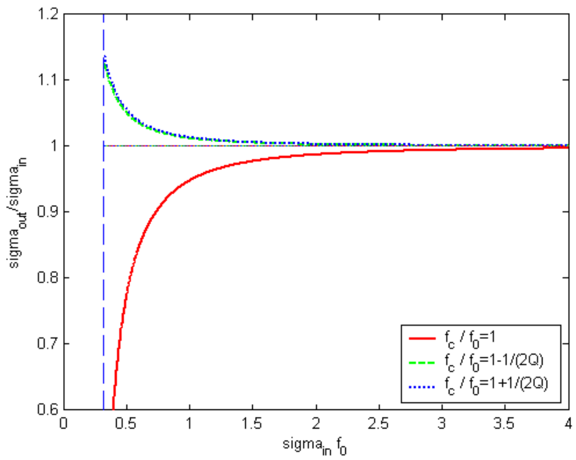

(*b*)

Figure 6: Graphs of (a) group delay and (b) standard deviation as a function of initial pulse duration for χ_{DC}=0.001 and Q=10.

5 Numerical Results- Propagation at 60GHz

To demonstrate the described approach we analyze the transmission of ultra short pulses in the 60GHz band. The high atmospheric attenuation and dispersive effects, caused by the absorption of the oxygen molecules at this frequency region [11-14], are expressed as evident distortions on the pulse delay, duration and shape.

The procedure, following the flow chart of Figure 3, was employed in a numerical program aimed at the simulation of pulse transmission in the atmosphere. In our study, the modulating base-band signal $A_{in}(t)$ was taken to be Gaussian. The initial standard deviation σ_{in} of pulse duration was varied, examining its effect on the resultant pulse envelope $A_{out}(t)$ along the path of propagation.

Examination of the approximated analytical expression obtained for t_d in the preceding section, discloses that the first order derivative α' of the attenuation coefficient plays a role in determining the pulse delay. Its major effect on increasing of the group delay is observed in Figure 7.*a*. in the vicinity of the frequencies 56.5GHz and 63GHz, where the most negative values of the product $\alpha'\beta''$ are obtained. Minimum delay is obtained at 60.5GHz where $\alpha'=0$ as expected.

The frequency dependent standard deviation is shown in Figure 7.*b* for several initial pulse widths σ_{in}. In this example, a pulse with initial duration of σ_{in}=0.2nsec is shown to be shortened ($\sigma_{out}/\sigma_{in}<1$) at frequencies where $\alpha''<0$, satisfies conditions for compression.

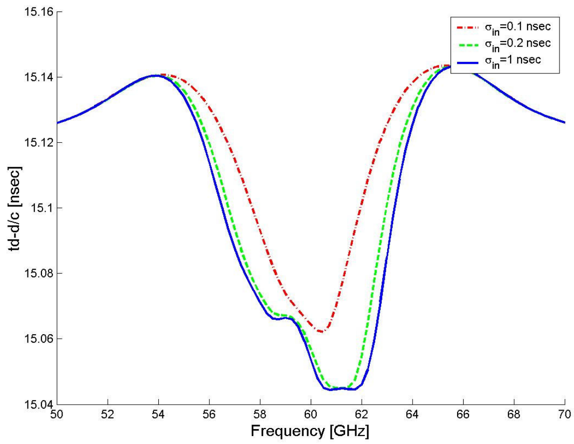

(*a*)

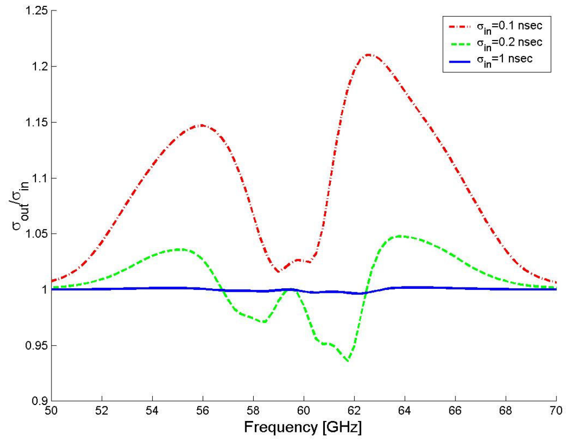

(*b*)

Figure 7: Graphs of (*a*) group delay and (*b*) standard deviation vs. frequency after a pulse propagation distance of *d*=1Km

6 Conclusion

Atmospheric transmission of millimeter waves, modulated by ultra-short Gaussian pulses, is studied analytically and numerically in the frequency domain revealing spectral effects on pulse propagation delay, width and distortions. Using second order expansion of the propagation factors leads to the derivation of approximated analytical expressions for the delay and width as a function of distance and carrier frequency. Conditions under which pulse compression or expansion occurs were identified.

By studying propagation of a pulse in the atmosphere, characterized by the millimeter-wave propagation model (MPM), it was shown that even in a medium of atmospheric air some of the effects that we predict are pronounced especially for carrier frequencies in the vicinity of the 60GHz, where high absorption of oxygen molecules occurs.

References:

[1] R.K. Crane, "Propagation phenomena affecting satellite communication systems operating in the centimeter and millimeter wavelength bands", *Proc. of the IEEE*, 59, (2), (1971), 173-188

[2] R.K. Crane, "Fundamental limitations caused by RF propagation", *Proc. IEEE*, 69, (2), (1981), 196-209

[3] L.J. Ippolito, "Radio propagation for space communication systems", *Proc. IEEE*, 69, (6), (1981), 697-727

[4] H.J. Liebe, "Atmospheric EHF window transparencies near 35, 90, 140 and 220 GHz", *IEEE Trans. On Antennas and Propagation*, 31, (1), (1983), 127-135

[5] R.A. Bohlander, R. W. McMillan: "Atmospheric effects on near millimeter wave propagation", *Proc. Of the IEEE*, 73, (1), (1985), 49-60

[6] N.C. Currie, and C.E. Brown, *Principles and applications of millimeter-wave radar*, Artech House (1987)

[7] H. J. Liebe, "An updated model for millimeter wave propagation in moist air", *Radio Sci*., 20, (1985), 1069-1089

[8] H.J. Liebe, "MPM – An atmospheric millimeter-wave propagation model", *Int. J. of Infrared and Millimeter waves*, 10, (6), (1989), 631-650

[9] H.J. Liebe, T. Manabe and G.A. Hufford, "Millimeter-wave attenuation and delay rates due to fog / cloud conditions", *IEEE Trans. On Antennas and Propagation*, 37, (12), (1989), 1617-1623

[10] H.J. Liebe, G.A. Hufford and T. Manabe, "A model for the complex permittivity of water at frequencies below 1THz", *Int. J. of Infrared and Millimeter waves*, 12, (7), (1991), 659-675

[11] J.H. van Vleck, "The absorption of microwaves by oxygen", *Phys. Rev.*, 71, (1947), 413-424

[12] P. W. Rosenkranz, "Shape of the 5 mm oxygen band in the atmosphere", *IEEE Trans. On Antennas and Propagation*, 23 (1975), 498-506

[13] H.J. Liebe, P. W. Rosenkranz and G.A. Hufford, "Atmospheric 60GHz oxygen spectrum: new laboratory measurements and line parameters", *J. of Quantitative Spectroscopy and Radiative Transfer*, 48, (1992), 629-643

[14] F. Giannetti, M. Luise and R. Reggiani, "Mobile and personal communications in the 60GHz band: a survey", *Wireless Personal Communications*, 10, (1999), 207-243

[15] Y. Pinhasi, A. Yahalom, O. Harpaz and G. Vilner, "Study of ultra wideband transmission in the extremely high frequency (EHF) band", *IEEE Trans. On Antennas and Propagation*, 52 (2004), 2833-2842

[16] Y. Pinhasi and A. Yahalom, "Spectral Characteristics of Gaseous Media and Their effects on Propagation of Ultra-Wideband Radiation in the Millimeter Wavelengths", *J. Non-Cryst. Sol.*, 351, (2005), 2925-2928

[17] Y. Pinhasi, A. Yahalom and G.A. Pinhasi, "Propagation Analysis of Ultra-Short Pulses in Resonant Dielectric Media", *J. Opt. Soc. Am. B*, Vol. 26, No. 12/December 2009

Yosef Pinhasi is the Dean of the Faculty of Engineering at the Ariel University of Samaria. He was born in Israel on May 3, 1961, received the B.Sc., M.Sc. and Ph.D. degrees in electrical engineering from Tel-Aviv University, Israel in 1983, 1989 and 1995 respectively. He served as the head of the Department of Electrical and Electronic Engineering between the years 2004-2007.

Since 1990 he is working in the field of electromagnetic radiation, investigating mechanisms of its excitation and generation in high power radiation sources like microwave and millimeter wave electron devices, free-electron lasers (FELs) and masers. He developed a unified coupled-mode theory of electromagnetic field excitation and propagation in the frequency domain, enabling study of wideband interactions of electromagnetic waves in media in the linear and non-linear (saturation) operation regimes.

Prof. Pinhasi investigates utilization of electromagnetic waves in a wide range of frequencies for various applications such as communications, remote sensing and imaging. The space-frequency approach, which developed by him, is employed to study propagation of wide-band signals in absorptive and dispersive media in broadband communication links, and wireless indoor and outdoor networks as well as in remote sensing Radars operating in the millimeter and Tera-Hertz regimes.
http://www.ariel.ac.il/sites/yosip/

Asher Yahalom is an Associate Professor in the Faculty of Engineering at the Ariel University Center of Samaria and the Academic director of the free electron laser user center which is located within the University Center campus. He was born in Israel on November 15, 1968, received the B.Sc., M.Sc. and Ph.D. degrees in mathematics and physics from the Hebrew University in Jerusalem, Israel in 1990, 1991 and 1996 respectively. Asher Yahalom was a postdoctoral fellow (1998) in the department of electrical engineering of Tel-Aviv University, Israel. In 1999 he joined the faculty of the Ariel University Center of Samaria. During the years 2005-2006 he was a Senior Academic Visitor in the University of Cambridge, Cambridge, UK. Details can be found in:
http://www.ariel.ac.il/sites/ayahalom/

Gad Pinhasi is a senior lecturer in the Faculty of Engineering at the Ariel University Center of Samaria, at the Department of Chemical Engineering and Biotechnology. He was born in Israel on August 4, 1963, received the B.Sc., M.Sc. degree from Ben-Gurion University of the Negev and Ph.D. degree from Tel-Aviv University Israel, all in mechanical engineering, in 1990, 1993 and 2001 respectively.

Since 2001 he is working in numerical analysis and computational fluid dynamics, investigating mechanisms of two-phase flashing flow. He developed a novel model for predicting the thermodynamic and the dynamic state of the boiling liquid during a boiling liquid expanding vapor explosion (BLEVE) event.
http://www.ariel.ac.il/sites/gadip/